PROSTHETICS

Excitation of natural spinal reflex loops in the sensory-motor control of hand prostheses

Patrick G. Sagastegui Alva[1]*, Anna Boesendorfer[2], Oskar C. Aszmann[2,3], Jaime Ibáñez[1,4]*†, Dario Farina[1]*†

Sensory feedback for prosthesis control is typically based on encoding sensory information in specific types of sensory stimuli that the users interpret to adjust the control of the prosthesis. However, in physiological conditions, the afferent feedback received from peripheral nerves is not only processed consciously but also modulates spinal reflex loops that contribute to the neural information driving muscles. Spinal pathways are relevant for sensory-motor integration, but they are commonly not leveraged for prosthesis control. We propose an approach to improve sensory-motor integration for prosthesis control based on modulating the excitability of spinal circuits through the vibration of tendons in a closed loop with muscle activity. We measured muscle signals in healthy participants and amputees during different motor tasks, and we closed the loop by applying vibration on tendons connected to the muscles, which modulated the excitability of motor neurons. The control signals to the prosthesis were thus the combination of voluntary control and additional spinal reflex inputs induced by tendon vibration. Results showed that closed-loop tendon vibration was able to modulate the neural drive to the muscles. When closed-loop tendon vibration was used, participants could achieve similar or better control performance in interfaces using muscle activation than without stimulation. Stimulation could even improve prosthetic grasping in amputees. Overall, our results indicate that closed-loop tendon vibration can integrate spinal reflex pathways in the myocontrol system and open the possibility of incorporating natural feedback loops in prosthesis control.

INTRODUCTION

The loss of a limb directly affects both efferent and afferent pathways. Modern prosthetic devices for amputees aim to establish reliable bidirectional human-machine interfaces for restoring sensory-motor control. The decoding of the neural inputs to limbs (*1*) and muscles has improved substantially during the past years, boosting the control and functionality of prostheses (*2*, *3*). However, to further improve prosthetic control, it is necessary to also restore afferent pathways sending sensed information in the periphery back to the central nervous system (*4*–*6*). Restoring these natural sensory inputs is a major challenge, with important current limitations (*7*, *8*).

Recent advances in upper limb prostheses have led to promising developments in noninvasive sensory feedback techniques, enhancing functionality and user experience (*9*–*13*). These techniques, such as sensory substitution or remapping (*10*–*19*), involve encoding prosthetic device parameters through different stimulation patterns of the stump (*12*, *20*). The aim is to convey information about the prosthesis state to the user through preserved sensory pathways that would send different information to an unaffected limb (*12*, *21*). Different types of sensory information can be transmitted to the prosthesis user in this way. For instance, force feedback, achieved through sensor-detected prosthesis force, grants users tactile and pressure sensations (*4*). Similarly, mechanotactile feedback, using pressure sensors (*22*), mimics natural limb sensations by applying pressure to specific areas of the stump. Bone conduction harnesses skull bone vibrations to provide sound and vibration feedback (*23*) about the prosthesis. These noninvasive and invasive sensory feedback techniques can collectively enhance upper limb prosthetic functionality, offering touch, pressure, and sound sensations that improve control and object manipulation (*11*, *12*, *16*, *20*, *24*). Such improvement suggests potential enhancements through task-specific information utilization (*9*, *24*). However, achieving these improvements poses challenges. Sensory substitution relies on the participant's ability to process and interpret the perceived feedback information while in motion and to adapt the motor commands sent to the prosthesis according to the received information (*19*, *21*, *25*). This makes the control of the prosthesis a complex task that can be cognitively demanding. Emerging modalities are exploring sensory fusion to maximize information transmission to the nervous system (*9*, *26*), combining kinesthesia, touch, and motor intent for comprehensive sensory-motor restoration (*27*). Alternatively, natural feedback, in terms of sensations perceived by the user, may be partly achieved by direct nerve stimulation (*25*, *28*–*31*), requiring invasive electrode implants. Although invasive technologies offer a homologous natural sensation to convey information about the prosthesis and its interaction with the environment, their main working principle still involves the cognitive processing of sensory inputs (*25*, *27*, *31*).

Although providing interpretable sensations is of great importance for sensory-motor control (*32*, *33*), sensory feedback in natural movements not only has the role of informing the somatosensory cortex but also is projected, mono- or polysynaptically, to spinal motor neurons and spinal interneurons, influencing their activity (*34*–*36*). These projections play a fundamental role in motor control by contributing to the modulation of the excitability of pools of motor neurons (*37*–*39*). Moreover, sensory processing in spinal pathways is beneficial in promptly compensating for disturbances in motor control by automatically generating correcting responses to the muscles in the

[1]Department of Bioengineering, Imperial College London, London, UK. [2]Clinical Laboratory for Bionic Extremity Reconstruction, Department of Plastic, Reconstructive and Aesthetic Surgery, Medical University of Vienna, Vienna, Austria. [3]Department of Plastic, Reconstructive and Aesthetic Surgery, Medical University of Vienna, Vienna, Austria. [4]BSICoS group, I3A Institute, University of Zaragoza, IIS Aragón, Zaragoza, Spain.
*Corresponding author. Email: pgs17@ic.ac.uk (P.G.S.A.); jibanez@unizar.es (J.I.); d.farina@imperial.ac.uk (D.F.)
†These authors contributed equally to this work.

presence of external perturbations [for example, mechanisms for posture stabilization during grasping control (*40*–*42*) or prevention of excessive stretch (*43*)]. These pathways are commonly preserved in amputees (*4*). Their stimulation could potentially be used to further enhance or modulate the motor commands used for prosthesis control in a similar way as sensory reflexes do in natural motor control (*44*, *45*). In this work, we designed artificial mechanical stimulation patterns that do not necessarily maximize the capacity of prosthetic users to cognitively interpret and discriminate different stimuli; rather, we propose patterns of stimulation that maximize the stimulation effect on the activity of spinal motor neurons, that is, stimuli that target the natural sensory-motor spinal loops. This perspective in providing feedback focuses on spinal integration of the feedback and on the involuntary (rather than voluntary) adjustments in motor neuron output (that is, the control signal of the prosthesis) as a consequence of the provided feedback. This key difference with respect to classic sensory substitution provides a paradigm for feedback integration into prosthesis use that may restore or enhance natural sensory-motor pathways.

Mechanical vibration over the muscle tendon has been previously explored to provide illusory kinesthetic perception (*35*, *46*) by excitation of muscle spindles. This technique has been exploited to convey proprioceptive information related to grip movements during prosthetic control (*4*, *27*, *45*). In addition, the tendon vibration induces a secondary mechanism that actively modulates the excitability of the motor neurons innervating the stimulated muscle (*38*); this effect is known as the tonic vibration reflex (TVR). The vibratory stimulation activates type Ia and type II sensory afferents (*47*–*49*) that generate excitatory inputs to the motor neurons controlling the stimulated muscles (*39*, *50*). The firing impulses are interpreted at the spinal level as if the muscle is stretched, producing a further increase in muscle activation (*51*). Concurrently, this process tends to induce a reciprocal relaxation response in the antagonist muscle that opposes the one undergoing vibration (*47*). Enhancement of this reflex effect has not been investigated in the context of prosthetic applications, perhaps because of concerns about a possible negative influence of stimulation on the volitional modulation of motor outputs (*4*). Nonetheless, modulation of motor output by spinal loop pathways is the physiological working condition for the central nervous system that adjusts the supraspinal drive to motor neurons according to the integration of sensory feedback (*40*). The motor neuron output is then the combination of voluntary and sensory drive to the motor neurons (*52*). Because the motor neuron output is the drive to the muscles that are then used for the prosthetic control, the sensory-motor loop is closed by the activated prosthesis in the same way as during natural muscle control.

In this study, we investigated the integration of the TVR to modulate muscle activity and its integration with myoelectric control, creating a comprehensive sensory-motor closed-loop system. The aim was to interface reflex sensory-motor loops by modulating the afferent input to motor neurons during concomitant voluntary control in a myocontrol task. This modulation integrates natural mechanisms, such as corrective responses or afferent support for muscle activation (*40*), into prosthesis control. Some of these types of disturbance corrections can be achieved by endowing the prosthesis with greater intelligence and autonomy (*53*, *54*), including the implementation of mechanisms such as anti-slip features (*55*, *56*), adjusting thresholds, and gains at the software level (*57*). However, enhancing prosthesis autonomy to handle disturbances comes with the potential drawback of diminishing overall embodiment and reducing the user's perception of prosthetic control (*58*). In our present study, we aimed to establish an interaction that targets task-related neural activity and that aligns with voluntary control, thus alleviating potential concerns inherent in automatic software implementation regarding lack of embodiment and ownership and preserving the user's sense of control throughout the integration process.

Our hypothesis is that adding reflex loops to the closed-loop control of a prosthesis would positively influence prosthetic control by mimicking natural sensory-motor interaction at the spinal level. As a representative approach that modulates the afferent input to motor neurons, we explored the best conditions to evoke and control the TVR by fine-tuning the stimulation parameters. We propose two closed-loop modalities to integrate this reflex mechanism in sensory-motor control for able-bodied (AB) participants and transradial amputees (TAs). For amputees, the system was fully integrated into real prosthesis control during activities of daily living.

RESULTS

Physiological integration of tendon vibration reflex in sensory-motor control

In our studies, we focused on stimulating the flexor muscles of the forearm, specifically targeting the muscle-tendon ends. The aim was to elicit activity in the muscle spindles and to evaluate the concept of artificially triggering the spinal reflex loops in a closed loop with muscle activity. A band-strap tactor (see Materials and Methods) was placed on the flexor common tendons of each participant to target the flexor muscle spindles. The vibration of the muscle tendon induces activity in Ia fibers innervating the stimulated muscles and projecting to the spinal cord (Fig. 1) (*59*, *60*). The induced activity in the afferent projections has an excitatory effect on the motor neurons of the stimulated muscle via a monosynaptic reflex pathway. The tendon vibration also typically induces a reciprocal relaxation response in the antagonist muscle opposing the one undergoing vibration. However, for the purpose of this study, our focus here was on the excitatory effects of the stimulation. The afferent input is a result of the muscle stimulation, combined with other spinal and supraspinal inputs to motor neurons, which integrate these received synaptic inputs and discharge action potentials that reach the muscle, ultimately determining its level of contraction. The overall myoelectric activity generated by the muscles (flexor carpi radialis, FCR) of the participants is the result of the combination of voluntary commands generated by the user and the afferent feedback, which includes the modulatory effects of the tendon vibration. This physiological integration of voluntary and sensory inputs is expected to mimic natural reflex mechanisms, adapting muscle activity for specific tasks and forming a reinforcing positive loop to enhance muscle activation, similar to natural sensory-motor closed loops (*33*), thus promoting improvements in control and embodiment.

Figure 1 (TVR evaluation framework) schematically shows the experiments conducted from basic physiological investigations of the TVR to functional tests with prostheses. The experiments aimed to evaluate the viability of incorporating the TVR in sensory-motor control with the goal of improving and refining muscle contractions during prosthetic operation. For this purpose, we first conducted three physiological experiments and then explored the potential functional benefits of our proposed approach in two additional tests involving the control of a prosthetic hand. The first physiological test

ERRATUM PUBLISHED 31 JULY 2024; SEE FULL TEXT

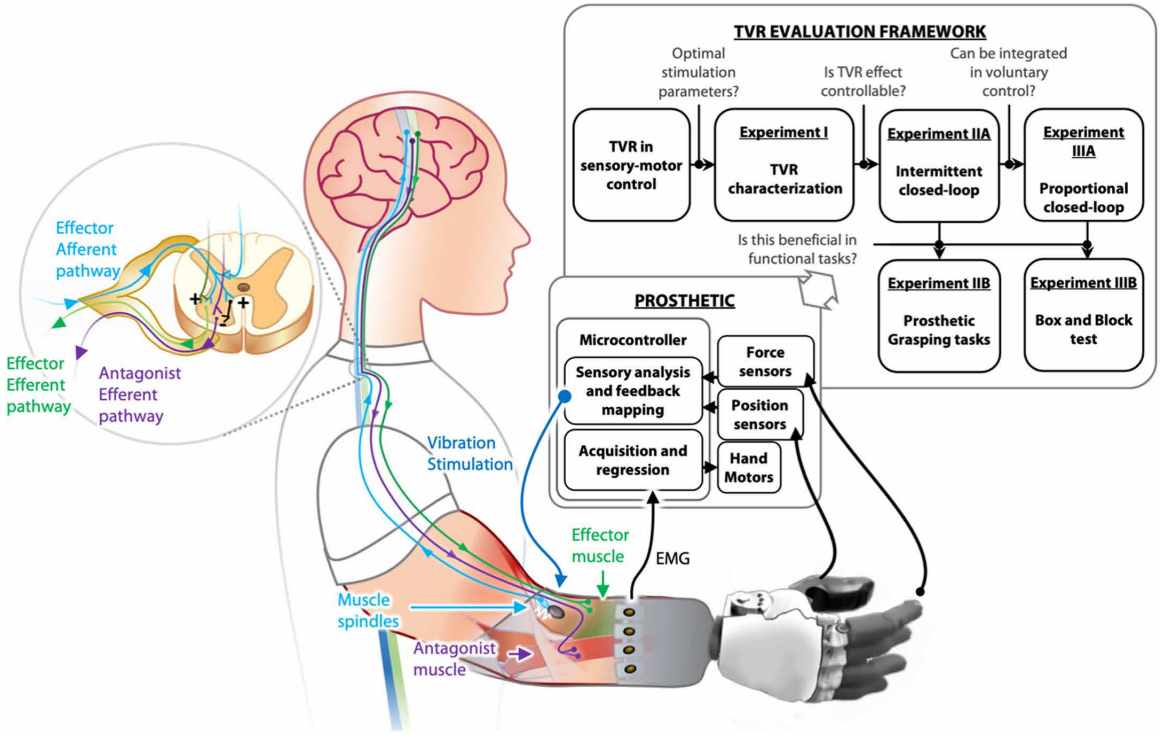

Fig. 1. Concept for the afferent spinal closed-loop integration for sensory-motor control and evaluation framework. Muscle tendon stimulation (dark blue arrow) elicits activity in muscle spindles modulating afferent inputs to motor neurons via a spinal reflex arc (light blue arrow). The integrated set of neural inputs to motor neurons (including the evoked afferent activity) determines muscle contraction by modulating the level of activity in the agonistic efferent input purple arrow). This scheme allows direct modulation of motor outputs (muscle activity) for prosthesis control via a spinal cord–mediated artificial loop. The top-right box summarizes the experiments performed to test the proposed closed-loop scheme for prosthetic control. Three physiological experiments (I, IIA, and IIIA) evaluated the TVR effects during contraction periods and participants' ability to integrate the TVR effects in their volitional control of muscle activation. Two functional experiments (IIB and IIIB) assessed potential benefits in real-life scenarios in amputees.

aimed to characterize the influence of the stimulation frequency on the elicited TVR response (experiment I). This allowed us to identify participant-specific optimal stimulation frequencies to effectively induce TVR effects. Then, we investigated the feasibility of controlling the TVR effect in a closed loop by intermittently enabling and disabling it on the basis of the recorded muscle activity (experiment IIA). Demonstrating the controllability of these effects allowed us to adjust in a closed loop the motor output activity to reach specific reference levels. Last, we assessed the integration of the TVR effect into voluntary control (experiment IIIA). This evaluation involved stimulating through a proportional closed-loop approach, where the level of stimulation (amplitude of the vibration) was proportionally controlled on the basis of the recorded muscle activity. This test combined the closed-loop stimulation (acting as a positive feedback loop with muscle activation) with the volitional adaptation of muscle activity by the participants, and it allowed us to test whether the closed-loop stimulation could be successfully integrated by the participants to perform a target tracking task with the level of muscle activity. By showing that this stimulation condition did not disrupt performance, we were able to show that closed-loop TVR could be integrated into voluntary control. Having established the feasibility of controlling and integrating TVR into sensory-motor control, the last two experiments (experiments IIB and IIIB) were done to determine whether the tested closed-loop TVR framework could lead to functional benefits in the control of a prosthetic device.

Experiment I: Physiological characterization to optimally induce TVR effects

We first evaluated the relevance of the stimulation frequency on the elicited TVR responses. In this initial part, we aimed to identify, on a participant-by-participant basis, the stimulation frequencies that elicited the highest TVR effects and tested whether the induced force modulation [or electromyographic (EMG) amplitude modulation] changed with the stimulation amplitude. Previous studies have reported maximum TVR effects at vibration frequencies from 80 to 160 Hz and stimulation amplitudes close to 1 mm (*47*–*49*, *61*). However, the reported frequencies and amplitudes that evoke the highest EMG responses vary greatly across participants and studies. This is due to the different setup strategies or stimulation conditions tested and the complexity of measuring the actual force exerted on the tendon.

Participants were asked to perform isometric wrist flexions with the application of force with the palm of the hand to an isometric force measurement platform. The force and EMG exerted by the palm were recorded to track changes in the generated force output. The root mean square (RMS) of the EMG signal was calculated and then normalized using resting and maximum voluntary contraction

(MVC) EMG levels. These normalized RMS EMG values, representing the contraction level, are denoted as NormEMG. Participants received visual feedback in the form of NormEMG to inform them about their muscle contraction level. Initially, participants were instructed to attain a 10% NormEMG level during an isometric wrist flexion task while receiving visual feedback. After the participant reached the requested level of contraction, the visual feedback was disabled, and the participant was instructed to keep the same level of contraction for 20 s without visual feedback. After 5 s, the stimulation was enabled for 10 s at 80, 100, 120, or 140 Hz. A control condition with an identical task without the stimulation was also added. The difference in the average NormEMG measured from the FCR at the beginning and end of the stimulation period (ΔEMG) was used to quantify the TVR effect on the motor output of the participants.

The changes in force (ΔF) and ΔEMG during the stimulation phase are displayed in Fig. 2A for all AB participants. In both measurements, an initial transitory phase followed by a steady-state phase could be observed, suggesting a cumulative effect of the TVR over time. For all frequencies tested, the steady state was reached within the first second after stimulation. Overall, there was an increase in the force produced and in the NormEMG for all participants (both AB and TA) for most stimulation frequencies. There was a significant increase in the ΔEMG level at the end of the blocks (relative to the NormEMG level before the stimulation started) for the cases in which stimuli were given at 100 Hz (2.66 ± 2.41%), 120 Hz (2.35 ± 3.40%), and 140 Hz (2.97 ± 4.02%) compared with the no-stimulation condition (0.78 ± 2.14%) (Fig. 2B) ($P < 0.001$, $P < 0.01$, and $P < 0.001$, respectively). In accordance with previous studies (*62*–*64*), there was a positive correlation between the frequency of stimulation and the TVR effect. The frequencies leading to the highest effect on force were 120 and 140 Hz for both AB and TA participants. However, there was no significant difference in the effect produced by these two frequencies ($P = 0.311$). Figure 2C shows the maximum ΔEMG elicited during stimulation for each AB participant

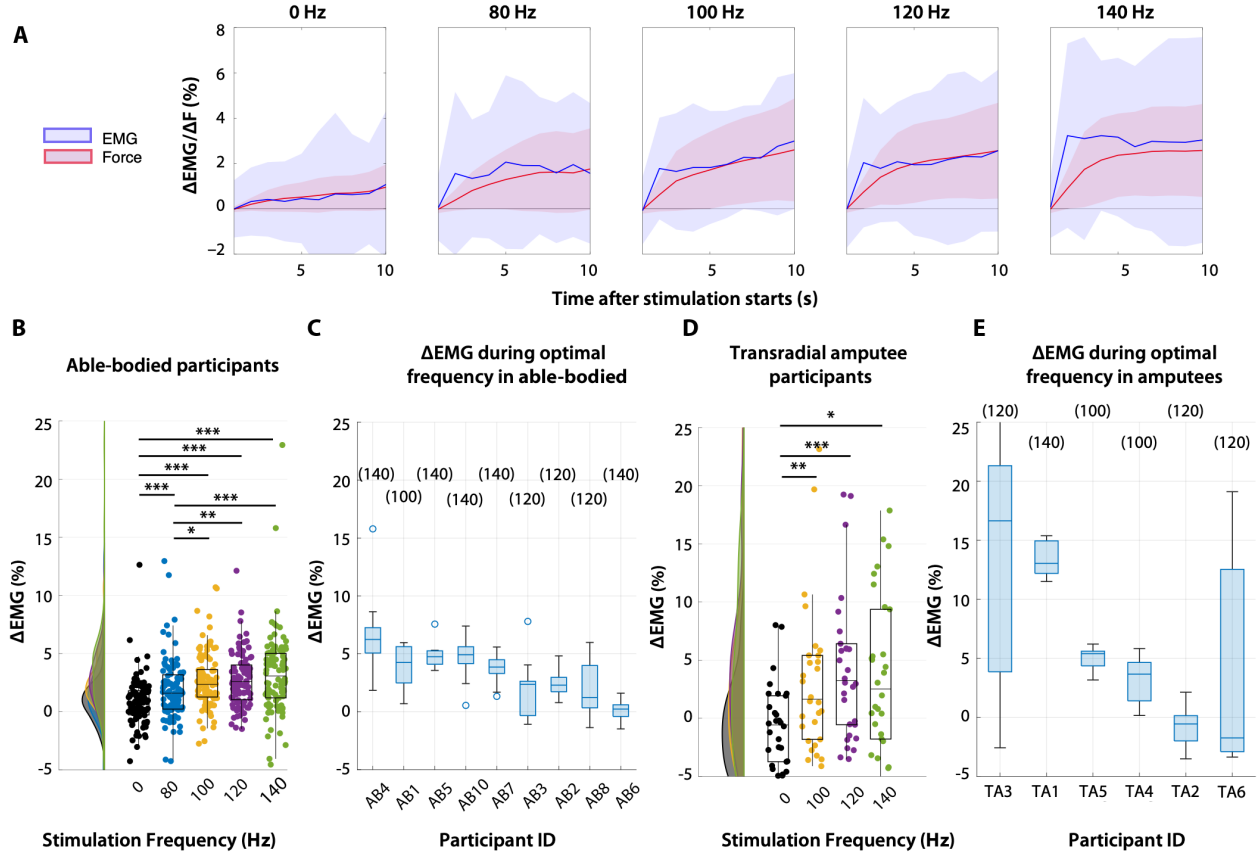

Fig. 2. Motor output drifts during stimulation and disabled tracking visual feedback. (**A**) Evolution of TVR effects on forces and EMG over time in AB participants ($n = 9$, trials = 90). The NormEMG is in blue, and the force is in red (traces and shades show the average and SD, respectively, across participants; $n = 9$; participants performed 10 trials per condition). (**B**) Density plots and individual measurements of the ΔEMG motor output across AB participants ($n = 9$; participants performed 10 trials per condition). Each sample (point) represents a single trial of the ΔEMG over 10 s between the beginning and the end of the stimulation period. (**C**) Overall optimal stimulation effects for each AB participant (10 trials performed per participant). The optimal stimulation frequency is noted in parentheses on top of each boxplot. Each sample represents the average ΔEMG during the stimulation time per trial. For this plot, the order in which participants are arranged on the *x* axis was based on the level of ΔEMG observed. (**D**) Density plots of the ΔEMG motor output in TA participants ($n = 6$; participants performed five trials per condition). Each sample (point) represents a single trial of the ΔEMG over 10 s between the beginning and the end of the stimulation period. (**E**) Overall optimal stimulation effects for each TA participant (five trials performed per participant). The optimal stimulation frequency is noted in parentheses on top of each boxplot. The order in which participants are arranged on the *x* axis was based on the level of ΔEMG observed.

for the optimal stimulation frequency. The frequency that elicited the maximum ΔEMG was selected as the optimal individual frequency for each participant.

For the TA participants (Fig. 2D), all frequencies evoked a significant positive drift. The frequency that led to the largest effect compared with nonstimulation (−0.57 ± 3.59%) was 120 Hz (3.23 ± 7.48%) ($P < 0.001$), followed by 140 Hz (2.51 ± 6.73%) ($P < 0.05$). The stimulation frequency with the smallest effect was 100 Hz (1.63 ± 7.89%) ($P < 0.01$). As in AB individuals, the higher the stimulation frequency, the higher the TVR effect. However, in this case, the plateau frequency was observed at 120 Hz (the optimal frequency was 140 Hz in one case, 120 Hz in three cases, and 100 Hz in two cases). These participant-specific optimal frequencies were used in the subsequent experiments to implement the sensory-motor integration (Fig. 2E).

Experiment IIA: Control of TVR effect through intermittent stimulation

In the first experiment, we observed that the TVR effect increased the motor output over time (Fig. 2A). To assess its applicability in sensory-motor control, we examined the potential to regulate the magnitude of the TVR effect online using a closed-loop framework. For this purpose, we integrated the TVR into the participant's sensory-motor control using an optimal intermittent closed-loop stimulation controller capable of activating and deactivating the TVR on the basis of the observed NormEMG level. We assessed the capacity of this intermittent closed-loop approach to drive the TVR effect by modulating the initial motor output activity of a participant to a desired level. Through this implementation, our aim was to harness spinal reflex circuits in real-world scenarios, to fine-tune limb contractions without the participants' involvement in specific tasks, and to compensate for the effect of external perturbations (*40*, *44*).

The optimal intermittent closed loop was implemented by minimizing the error between the exerted output NormEMG level produced by the participant and a given reference EMG amplitude level (Fig. 3A). On the basis of the error, the stimulation to elicit the TVR was controlled in an on-off fashion: It was activated when the measured NormEMG level was below the target and disabled when the measured level was above the target level. This design aimed to stabilize the participants' output NormEMG level at the reference level used as a target in the task. The stimulation frequency used to implement the optimal intermittent closed loop was the optimal frequency obtained from experiment I.

To assess the controllability of the TVR, we isolated its contribution from the participants' voluntary muscle control by deactivating visual feedback during the optimal intermittent closed-loop activation. Participants were instructed to maintain sustained isometric wrist flexion at an initial baseline target. Subsequently, we removed the visual feedback and initiated the optimal intermittent closed loop to adjust the motor output. Although we attempted to isolate the TVR effect from the voluntary control, the overall EMG output still included the drive generated by the participants to hold the contraction at a constant level (Fig. 3A). TVR controllability was evaluated by calculating the success rate (evaluated by the ratio of the RMS values between the current NormEMG and the target level) of the intermittent closed-loop stimulation in making the NormEMG activity track a certain target level.

We included a baseline condition to ascertain participants' peak performance potential within the experimental task. This condition and the target during the task were adjusted considering the participants' physical differences between AB and amputee individuals. We set a step target (0 to 10% NormEMG) and enabled visual feedback during the baseline for AB individuals. This provided insight into how they adapted their control to minimize errors between the signal and the target level. In contrast, amputee participants encountered a constant target with visual feedback disabled. This choice accounted for physiological differences: Amputees rely on distinct neuromuscular control and sensory cues, making rapid muscle activity changes challenging. A constant target (10% NormEMG) aligns with their control strategy, emphasizing proprioception because of limb absence and mimicking how they naturally stabilize limb position without continuous visual input. In addition, to ensure that the observed effects with the optimal intermittent condition were attributable to TVR, we included a suboptimal intermittent closed-loop condition. In this condition, the stimulus frequency was set at 40 Hz, a frequency not expected to induce a TVR effect (*63*, *64*). This condition allowed us to disentangle the effects induced by the TVR from the possible modulation of muscle contraction done by the participants when receiving intermittent stimulation.

For AB participants, the reference target used in the tasks in this experiment consisted of maintaining a stable level of muscle activation and then producing a step increase (from 10 to 15% NormEMG) in muscle activation (purple dotted line in Fig. 3B). We observed that the optimal intermittent closed loop could modulate the control variable to track the target level. An example of the measured NormEMG traces in one AB participant, AB6, is shown in Fig. 3B. The success rate in the baseline condition was 93.72 ± 22.57% across participants. This was significantly higher than the success rates with the optimal intermittent closed loop (87.84 ± 22.57%) ($P < 0.01$) and the suboptimal intermittent closed loop (65.58 ± 16.64%) ($P < 0.001$) (Fig. 3C). The relatively small difference in success rate between the baseline condition and the optimal intermittent one demonstrates that the optimal intermittent condition was able to partly compensate for the drop in performance due to the removal of the visual feedback by increasing the level of NormEMG activation via the TVR. The optimal intermittent closed loop led to significantly higher success rates than the suboptimal closed loop [$P < 0.001$], emphasizing the importance of using an adequate stimulation frequency for the tendon vibration. This result also implies that the outcomes achieved through the optimal frequency were a result of modulating the afferent feedback affecting motor neuron activity rather than just acting as an interpretable sensory cue for participants.

In the case of the amputee participants, overall (Fig. 3D), the success rate in maintaining the reference target with the optimal intermittent closed loop (63.70 ± 15.01%) was significantly higher than in the baseline condition (49.52 ± 16.78%) ($P < 0.01$). The success rate of following the target using the optimal intermittent closed-loop condition was also significantly higher than the success rate obtained using the suboptimal intermittent closed-loop condition (58.77 ± 21.12%) ($P < 0.05$). The suboptimal intermittent closed loop was able to improve the baseline results; however, these improvements were not significantly different. The individual trials for the TA participant TA1 during this task are depicted in Fig. 3E as an example. For the baseline and suboptimal intermittent closed-loop

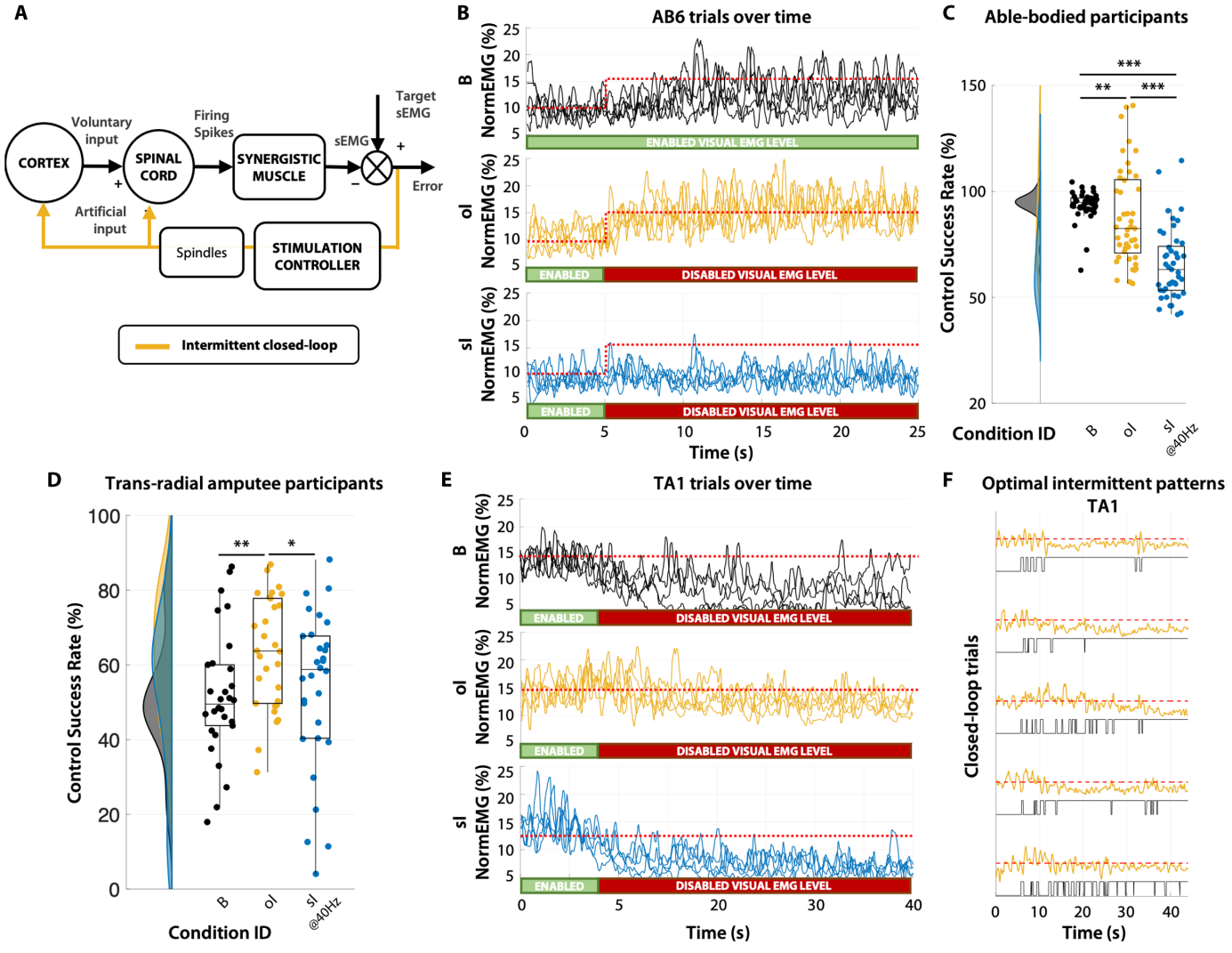

Fig. 3. Intermittent afferent closed-loop performance. (**A**) Concept of this reflex closed loop. The difference between a given EMG target and the actual EMG output of the participant is used to activate the stimulator and create a positive loop on the targeted muscle to reach the desired target. (**B**) Individual trials of a representative AB participant (AB6) in the baseline (B), optimal intermittent (oI), and suboptimal intermittent (sI) closed-loop stimulation conditions. Each subplot displays five trials conducted by the participant. The horizontal red dotted line represents the EMG target level that participants should generate. (**C**) Success rate for the control conditions across all AB participants ($n = 9$; each dot represents a single trial, and participants performed five trials per condition). (**D**) Success rate for the control conditions across all amputee participants ($n = 6$; dots represent individual trials, and participants performed five trials per condition). (**E**) Individual trials of a representative participant (TA1) for the baseline, oI, and sI closed-loop stimulation conditions. Each subplot includes the traces of the five trials conducted by the participant. The horizontal red dotted line represents the EMG target that participants were instructed to maintain throughout the trials. (**F**) Individual trials of a representative participant (TA1) for the oI closed-loop stimulation condition. The plots combine information about the EMG output (yellow traces) and the intervals of stimulation (black traces; low level, deactivated, and high level, activated).

conditions, the NormEMG tended to decrease after the visual feedback was disabled in all cases, leading to a reduction of the control success rates. The optimal closed-loop stimulation, on the other hand, was able to maintain a relatively stable output level during the whole trial. The individual patterns of activation for two participants (TA1 and TA2) are shown in Fig. 3F; the optimal closed-loop stimulation was able to modulate the NormEMG level without generating overshoots. Overall, the result from amputees indicates that the TVR reflex is also controllable in this population. Moreover, it suggests that even in scenarios with a low voluntary baseline, the optimally induced afferent spinal pathways can be used to actively modulate muscle activation in amputees.

Experiment IIB: Biomimetic object anti-slippage via an intermittent closed loop in amputees

To further assess the potential functional benefits of the intermittent closed-loop stimulation strategy tested in experiment IIA, we integrated this closed-loop method in the control of a prosthetic hand (Taska Prosthetics, New Zealand). The intermittent closed-loop stimulation strategy cannot be directly implemented in prosthesis control because of the absence of a predefined reference EMG trajectory. Nonetheless, a fundamental initial step in establishing the feasibility of integrating the TVR into sensory-motor control involved demonstrating its capability to modulate motor output effectively in tasks aimed at improving grasping. Moreover, simple

processing methods can be devised to estimate a reference EMG level, such as the EMG level shortly after contact.

After the preliminary study on force tracking, we conducted a grasping experiment. The object to grasp included a force sensor that allowed us to track the amount of force that the prosthesis was exerting. In these grasping tasks, we evaluated whether intermittent closed-loop control could improve the grasping stability, enabling the prolonged and controlled retention of an object with a consistent level of force. In this type of scenario, the participant should ideally exert a minimal range of force to avoid breaking the grasped object. To simulate this scenario, we displayed on the monitor a red visual sign when the grasping force exceeded a certain threshold to indicate the rupture of the object. This red sign and the visual inspection of the object were the only information given to the participant to hold it. The number of times that the object was dropped during the task was counted and used as a slipping indicator. To evaluate the effect of the intermittent closed-loop stimulation condition in this task, participants were requested to maintain a constant force on the object that was 20% of the maximum force that the prosthetic hand could exert. This percentage was determined through experimental pilot trials to ensure a stable grip. From the initial group of TA participants, only TA4, TA5, and TA7 were able to take part in this experiment because of time constraints in the conducted experimental sessions. The performance of the closed-loop conditions in assisting the participants to hold the object for prolonged periods was assessed by counting the number of drops and by measuring the average and SD of the exerted gripping force during the trial.

An example of the exerted force traces during the trials is shown in Fig. 4A. The average gripping force exerted was smaller in the optimal condition (42.05 ± 5.71%) than in the suboptimal condition (54.04 ± 12.90%), which indicates that the stimulation parameters have a relevant role in the assistance achieved with the stimulation (Fig. 4B, left). The differences in the exerted force between optimal and the baseline conditions followed a similar trend, with the baseline condition resulting in a higher force level applied to the object (46.52 ± 13.99%). The SD of the exerted force (Fig. 4B, right) was also lower in the optimal condition (27.31 ± 5.01%) than in the suboptimal (29.72 ± 5.13%) and baseline conditions (31.73 ± 6.34%). We could observe a decrease in the number of drops per trial, from 1.33 ± 0.98 drops per block to 0.50 ± 0.67 drops per block when the optimal intermittent closed loop was enabled (Fig. 4C). The suboptimal condition exhibited an intermediate performance level between the optimal and baseline conditions (1.08 ± 1.08 drops per block). These results reveal a reduction in the net exerted force alongside a decrease in its SD with the optimal stimulation condition. This was achieved while participants produced fewer drops in this condition than in the other two. These results suggest an improved performance in exerting lower-amplitude forces during the task during this optimal closed-loop condition. This improvement could potentially offer functional benefits by automatically adjusting the generated EMG command of the participant during tasks such as grasping.

Experiment IIIA: TVR afferent integration via proportional stimulation in voluntary control

The previous tests focused on controlling the tendon vibration stimulation using an intermittent closed-loop stimulation, regulating the on/off periods of stimulation. This strategy may be implemented during grasping, as exemplified in experiment II. However, for prosthetic myocontrol implementation, it is important to examine how the afferent input continuously integrates into a control loop, as in natural conditions. In this experiment, we evaluated whether the added afferent input disrupts the participant's overall voluntary control. For this purpose, we implemented a proportional closed-loop approach that superimposes the TVR afferent input onto voluntary activity.

The proportional closed-loop stimulation framework tested here adjusted the amplitude of the vibrators stimulating the tendon proportionally to the NormEMG (Fig. 5A). The stimulation frequency was fixed at the optimal value obtained in experiment I. The effects of the stimulation on motor neurons were superimposed onto the voluntary drive to the muscles generated by the participants to determine the overall level of muscle activation. This proportional control of the stimulation was meant to mimic natural sensory-motor closed loops, in which the input from primary and secondary afferents depends on the level of muscle activity (for example, on the control variable) and acts as positive feedback to support muscle activation (*36*, *64*).

Participants were asked to follow a reference EMG ramp trajectory to evaluate the influence of the stimulation on the produced

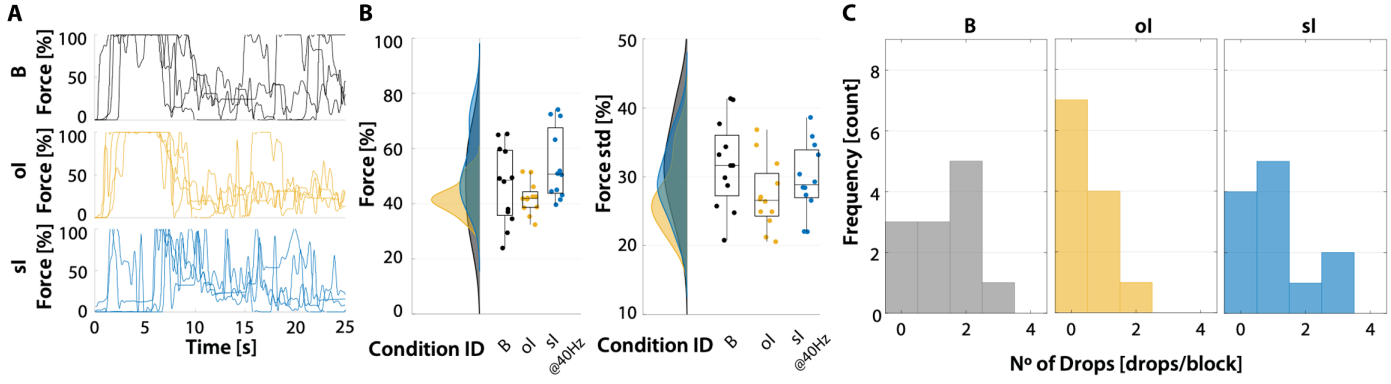

Fig. 4. Intermittent afferent closed-loop performance during prolonged object holding. (**A**) Individual trials of the exerted force by a representative participant (TA7) in the baseline (**B**), ol, and sl closed-loop stimulation conditions. Each subplot displays four trials conducted by the participant. (B) Means (left) and SD (right) of the gripping force exerted per trial for each stimulation condition across TA participants ($n = 3$; four trials performed per participant and condition). Dots represent individual trials. (**C**) Number of drops during prolonged object holding for all control conditions across TA participants, $n = 3$.

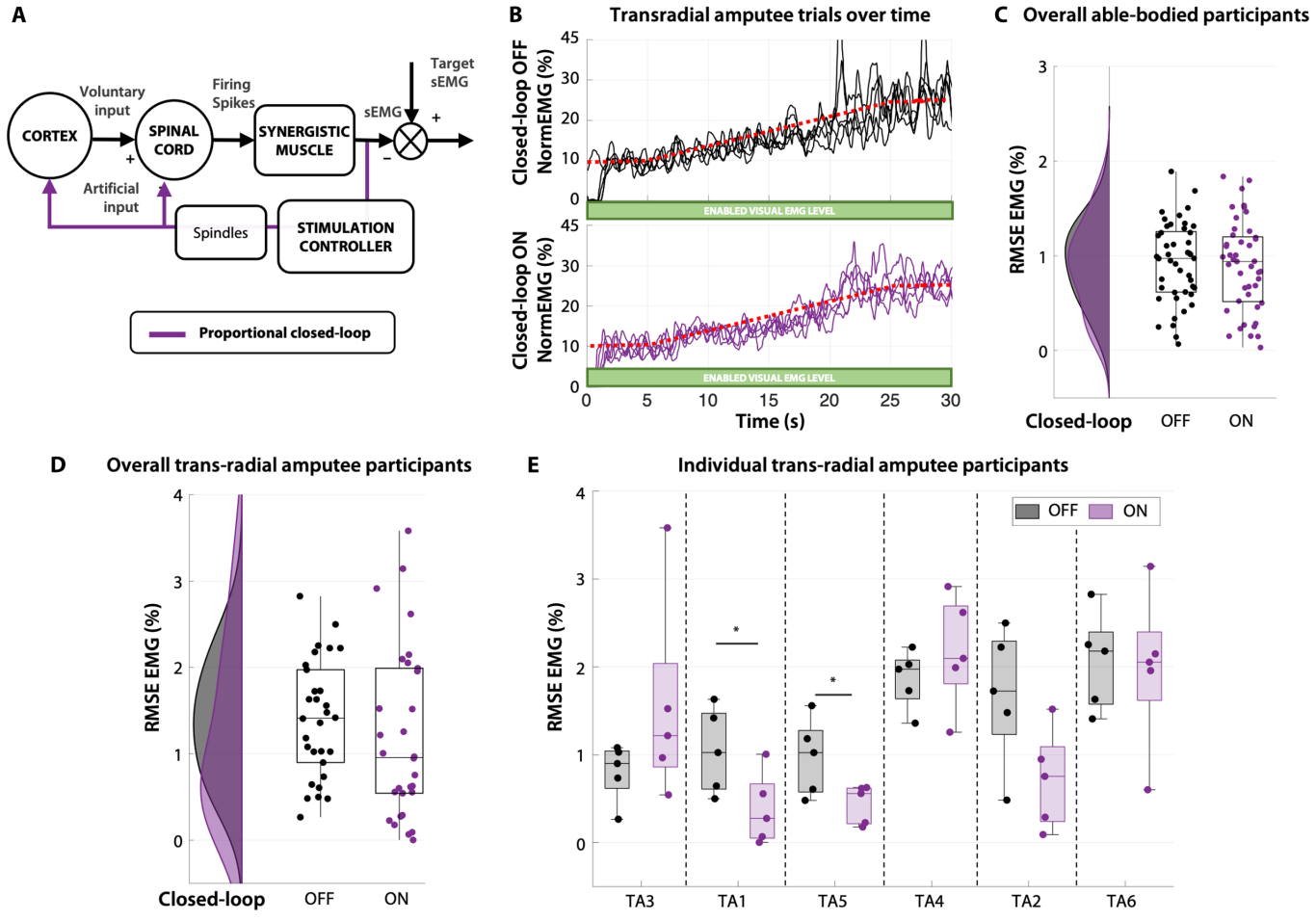

Fig. 5. Proportional closed-loop afferent effects superimposed to voluntary control. (**A**) Concept of the proportional closed loop: The exerted EMG envelope was proportionally mapped into the amplitude of stimulation to create a positive closed loop to modulate the excitability of the motor neurons innervating the target muscle. (**B**) Individual trials for TA1 following a ramp target with the proportional closed loop disabled (top) and enabled (bottom). The red dotted line indicates the ideal EMG target trajectory that the participant needs to voluntarily follow. Each subplot displays five trials conducted by the participant. (**C**) RMSE when following a target EMG trajectory with the proportional closed loop disabled (black) and enabled (purple) across all AB participants ($n = 9$; dots represent single trials; participants performed five trials per condition). (**D**) RMSE in trials performed by TAs following a target EMG trajectory with the proportional closed loops disabled (black) and enabled (purple) ($n = 6$; each dot represents a single trial, and participants performed five trials per condition). (**E**) RMSE measured from each TA participant with the proportional closed loop disabled (black) and enabled (purple). Participants performed five trials per condition.

EMG. The evaluation tasks involved tracking a ramp target at 0.75% per second for 20 s, starting at 10% NormEMG, mirroring the average EMG increase gradient seen in pilot experiments. After the slope, there was a 5-s plateau at 25% NormEMG (Fig. 5B). The performance in tracking the ramp while receiving the stimulation was compared with the performance achieved by the participants when they did the same task without receiving the stimulation (baseline condition). In both conditions, participants received visual feedback about their exerted NormEMG output to follow the ramp trajectory. The performance in following the trajectory was assessed by the RMS error (RMSE) between the reference ramp trajectory and the exerted NormEMG activity. Given the paradigm shift in this closed-loop stimulation, we conducted an additional evaluation (only reported in the Supplementary Materials) to verify the effectiveness of the proportional closed loop to induce TVR. This evaluation confirmed that the isolated contribution of this proportional closed-loop condition can elicit positive drifts in the motor output. These results are included in the supplementary methods (figs. S2 and S3).

The inclusion of proportional stimulation did not significantly affect the overall error made by the AB participants, and it remained comparable with the condition in which the stimulation was disabled ($P = 0.65$) (Fig. 5C). An increase in error would have been anticipated if the stimulation disrupted voluntary control. However, no increase or decrease was observed; the error remained at baseline levels. These findings indicate that the modulatory effects of the proportional closed-loop stimulation were successfully integrated by the AB participants. Having established the integration of sensory-motor control of AB individuals, our subsequent objective was to evaluate whether it could also be effectively integrated by amputees or even result in beneficial effects in their cases.

The average error (ramp + hold) across the six amputee participants was not significantly different (1.41 ± 0.95% to 0.95 ± 0.99%; $P = 0.24$) when the proportional closed loop was enabled (Fig. 5D). However, in two amputee participants (TA1 and TA5; Fig. 5E), the proportional closed-loop stimulation significantly decreased the

ERRATUM PUBLISHED 31 JULY 2024; SEE FULL TEXT

overall error (ramp + hold) to follow the trajectory from 1.02 ± 0.48% to 0.27 ± 0.41% ($P < 0.05$) and from 1.02 ± 0.33% to 0.55 ± 0.22% ($P < 0.05$), respectively. These findings indicate that the amputee participants integrated the modulatory effects of the proportional closed loop without any major perturbation in their voluntary control.

Experiment IIIB: Proportional afferent feedback during grasping in amputees

Given the results of the integration of a proportional stimulation into voluntary control in standardized conditions, we then aimed to add this feedback strategy in a more natural functional task, where the effects may not only be of effective integration but also of functional benefit. To evaluate the effect of the proportional closed-loop control on grasping dexterity during real-life object manipulation with a prosthetic, we conducted additional assessments using the targeted box and block test (*65*). The participants needed to move nine blocks from one compartment to another separated by a partition. Each block needed to be transported one by one in a specific order to a defined target location. The improvement in manual dexterity was evaluated by measuring the time needed to successfully transport all nine blocks from one compartment to the other. The number of times that the blocks fell during the task was also counted and used as a slipping indicator of the prosthesis control. Only participants TA2, TA4, TA5, and TA7 participated in this task because of time constraints in the experiments with the other participants. In the tested participants, although not significantly different ($P = 0.25$), we observed a decrease in the time needed to transport all the blocks when the proportional closed loop was enabled (Fig. 6A) to 51.08 ± 9.62 s (movie S1) compared with when it was disabled, 63.83 ± 23.22 s (movie S2). In addition, the number of total block drops per trial decreased from 0.91 ± 0.90 drops per block to 0.33 ± 0.65 drops per block when the proportional closed loop was enabled (Fig. 6B). The observed reduction in the time required to complete the task and in the number of drops among amputee participants in a functional task suggests the potential assistance provided by proportional closed-loop control in developing muscle contractions for transporting the blocks during the task.

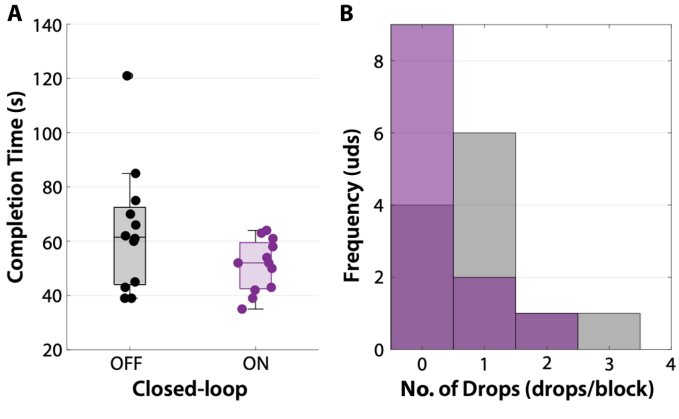

Fig. 6. Prosthesis control maneuvering with proportional closed loop. (**A**) Competition times and (**B**) histogram of number of drops for targeted box and block test when using Taska hand with the proportional closed loop disabled (black) and enabled (purple) across TA participants ($n = 4$; dots represent individual trials; participants performed three trials per condition).

DISCUSSION

Effective sensory-motor control requires the contribution of both supraspinal and spinal circuits to regulate the input to motor neurons controlling muscle activation. Here, we have proposed a framework for sensory feedback for prosthesis control based on the use of natural spinal reflex circuits. Our proposed framework aims to actively control the modulation of the afferent inputs to motor neurons. This becomes an additional source of synaptic input to spinal motor neurons modulating the output of the motor neurons. The output of the motor neurons then determines the level of muscle activity, which is used as a control signal, thus effectively closing the sensory-motor loop at the spinal level. To validate the concept, we present results involving both AB and amputee participants who performed various physiological and functional motor tasks. During these tasks, we applied tendon vibration in a closed-loop manner to modulate input to motor neurons, thereby influencing motor command through muscle activation. Results suggested that this stimulation can guide reflex changes in the motor neuron outputs to muscles and that participants can integrate this sensory input to adapt the motor commands to the muscles to ensure a correct motor performance.

We have proposed the control and integration of spinal reflex loops through peripheral sensory feedback to improve sensory-motor control in amputees. This approach facilitates corrective responses by modulating afferent inputs to motor neurons while preserving the users' voluntary input, thus maintaining a sense of control and ownership. This could potentially improve the overall control experience, making it more natural and intuitive compared with prostheses with automated functions for adjusting the forces produced. The approach has been validated with the TVR as a means to excite the sensory input to motor neurons. However, the same approach can be implemented with any other type of artificial stimulation of afferents, such as by direct nerve stimulation. For the control, we studied the afferent modulation of the motor output to mimic the reflex spinal circuits that fine-tune hand movements. For this purpose, we implemented an intermittent closed-loop paradigm that was able to actively modulate continuously the muscle output when the stimulation frequency was optimally selected for each participant. In addition, we assessed the integration of the reflex loop by proposing an afferent stimulation with an amplitude proportional to the voluntary commands, which aimed to establish a positive feedback loop with motor neurons. These different implementations of closed-loop stimulation were integrated into the sensory-motor control of the AB and amputee participants. In addition, integrating these closed-loop stimulation strategies into a prosthetic hand seemed to contribute to enhanced performance in functional tasks for amputees. The results demonstrated the possibility of controlling and integrating the TVR effects into sensory-motor closed loops, which may have positive effects on control performance and in prosthesis embodiment.

For the initial physiological characterization, in agreement with the literature, there was a positive correlation between the TVR effects and the frequency of stimulation. For this specific stimulation setup, 80 Hz had the lowest rate to elicit TVR effects, and the highest effects were observed in the range of 120 and 140 Hz for both AB and amputee participants. In (*63*), 150 Hz was found to be the upper threshold frequency to elicit TVR responses, which is similar to our upper limit of 140 Hz.

The intermittent closed-loop paradigm was able to control the effects of the TVR and actively modulated the EMG level in AB

participants and TAs in standard laboratory tests. As hypothesized, the functional effect on the AB participants was negligible, presumably because the control in these individuals was already optimal. Conversely, the intermittent strategy improved the overall performance of the amputees. The inclusion of the intermittent closed loop in the prosthetic system seemed to improve fine object manipulation during the functional tests in amputees. The participants had to maintain the grasp of an object without exceeding a threshold force level and without slippage of the object. This task requires the participant to maintain a steady muscle contraction for prolonged object holding, increasing slippage risk. The inclusion of the intermittent closed loop showed promise in maintaining a lower-amplitude force while reducing the number of drops, suggesting potential improvements in the stability and control of the prosthesis during object manipulation.

In a subsequent experiment, we successfully integrated the positive afferent input of the TVR during the proportional closed-loop stimulation paradigm. Increasing the algorithm gain typically boosts the EMG level while also amplifying its variability. However, in our data analysis, we observed that the integration of afferent feedback from TVR did not lead to an increase in EMG variability. The inclusion of this additional sensory feedback did not substantially affect the baseline voluntary performance of AB participants. Conversely, for TAs, the voluntary performance to follow the EMG targets tended to improve when the proportional closed loop was activated. In addition, the stimulation strategy used showed positive functional effects on the targeted box and block test. The positive feedback loop of the proportional sensory input appeared to amplify muscle contractions, resulting in a more stable grip as participants moved the blocks. This enhancement resulted in reduced completion times and a lower number of drops when the proportional closed loop was enabled. Although we suggest that this afferent input might activate spinal circuits affecting the neural inputs to muscles, potentially contributing to a gradual enhancement in the embodiment and intuitiveness of prosthetic device control, further investigation is warranted. Additional measurements, such as force exertion or control output, should be included in future studies using the targeted box and block test to appropriately assess and determine the functional improvement caused by the stimulation in this type of functional task.

Overall, the results demonstrated beneficial functional effects in incorporating spinal loops into closed-loop applications for prosthesis control. Unlike previous claims (*4*), when these loops are integrated and controlled in a closed loop, the resulting elicited reflexes can be effectively integrated and beneficial for the user. In optimal scenarios, the proportional addition of the afferent feedback to the voluntary command was able to improve the performance of participants to generate a certain level of muscle contraction. During afferent modulatory experiments, the intermittent closed loop was able to modulate the neural input to the motor neurons and modulate the overall muscle output to reach a certain force target. By fine-tuning this concept, the closed loop could be incorporated as a mechanism to modulate the grip command of the prosthesis and automatically regulate the force to apply to an object. This type of functionality is automated in some commercial prostheses using embedded sensors to regulate grip forces applied to an object (*66*). However, whenever these automatic functions are active, the user partially loses ownership of the overall grip because the internal microcontroller takes over the voluntary inputs of the user. This lack of control ownership decreases the user's feeling of embodiment (*22*). A similar effect would be felt if the proportional sensory input was added via software to the control signal rather than processed through the physiological integration at the motor neuron level. The potential benefit of the spinal feedback proposed here is that it could incorporate these automatic functions for grasping manipulation while maintaining a regulatory voluntary input from the user and with a natural integration of inputs that does not feel like an artificial change in the prosthesis commands. Moreover, this automatic mechanism engages the remaining muscles of the stump as they are being modulated by the spinal reflex closed loops. These findings suggest the potential effectiveness of the afferent closed loop in enhancing maneuverability and grip control during object manipulation, thereby contributing to improved functionality and usability of the prosthesis in real-world scenarios.

A limitation of the current study is the observed variability in the results among participants, which could be due to intrinsic or extrinsic factors of the stimulation interface. There are additional intrinsic stimulation factors besides those stated in this study that need to be addressed to tailor a stable interface. The stimulation point and area of stimulation are critical aspects to ensure the excitability of type Ia and type II sensory afferents. Moreover, the direct assessment of the Ia spinal reflex pathways, including tests like the Hoffmann reflex, would have been pivotal to confirming their role in eliciting the TVR. These additional measurements could have enhanced our understanding of the underlying mechanisms. Nevertheless, our experimental data complement existing literature, particularly within the selected stimulation frequencies known to induce a one-to-one response of muscle spindles. In this study, our primary focus was on the excitatory effect of the TVR. However, a comprehensive understanding of the effects of TVR on agonist-antagonist relations could potentially contribute to a better understanding of muscle coordination and interaction. In addition, an evaluation of the adaptability of these afferents to continuous stimulation needs to be assessed for long-term usage of these mechanisms in daily life for amputees. Ultimately, a direct selective nerve stimulation with electrode implants may result in a more specific activation with less variability across participants. The present work demonstrates a concept that can be translated in the future into more complex interfaces.

In conclusion, this study demonstrates the concept of integrating sensory feedback into natural spinal sensory-motor control closed loops. This approach naturally adds an involuntary component to the neural drive to the muscles that, in turn, generates the motor control signals for external devices. The method introduces a means to restore a continuous sensory contribution to the neural commands for external devices. These results may influence the performance and embodiment of prostheses.

MATERIALS AND METHODS

Study design

The study included two experimental sessions run on separate days for AB participants. Upon analyzing the results of the AB participants, the experimental protocol was adapted to the TAs by reducing the total experimental duration to 1 day. The experiments included 10 AB participants (four males and six females, average age

25.8 ± 4.6 years) who were all right-handed. In addition, six TAs (two females and five males, average age 41.28 ± 13.91 years) were recruited. TA1 had actively used a prosthetic for 4 years but ceased using it in the past 2 years. The remaining participants were current prosthetic users. Table 1 summarizes the information regarding the year of amputation, amputation level, and prosthetic usage. Because of time constraints, not all TA participants were able to complete the functional tasks. Informed consent was obtained from all participants before the experiments. The experimental procedure was approved by the Imperial College Research Ethics Committee (reference number 18IC4685).

Reflex-induced feedback and recording interface

During the experimental sessions, AB participants were seated comfortably in front of a table with a bilateral force platform that restricted the forearm and hand of both arms of the participants. The platform was designed to measure isolated isometric flexion forces with the wrist (Fig. 7A). Both forearms were positioned parallel on a desk with elbows at a 120° angle. The palms of both hands were placed on the center of the hand rests and secured with Velcro belts, with palms perpendicular to the desk (wrists at 90° to the desk).

Tendon vibration was induced using a C2-HDLF tactor (Fig. 7B; Engineering Acoustics Inc., USA). This device allowed independent control of stimulation frequency and displacement amplitude. It could operate at frequencies up to 200 Hz, with amplitudes ranging from 0.6 to 1.3 mm (fig. S1). To measure perpendicular forces between the stimulator tip and the skin, the tactor was modified to include an internal force sensor (FlexForce A101, Tekscan Inc., USA) (Fig. 7B). The stimulator was placed on the dominant arm's common flexor tendon using a soft strap to prevent vibration from affecting other muscles (Fig. 7E), with a contact force of approximately 2 N. The tendon location was determined through palpation while the participant performed wrist flexion. In pilot tests, we found higher effects when the stimulation was delivered at the proximal end rather than at the distal end of the muscle. In addition, the proximal end is the only area available for stimulation in amputees. Therefore, stimulation of the proximal end was used in all of our tests.

For AB participants, the surface EMG activity of their FCR was acquired using a tabletop amplifier (OT Quattrocento, OT Bioelettronica, Italy). Bipolar electrodes with a 2-cm interelectrode distance along the FCR were used to capture the surface EMG signals. The EMG data were sampled at 2048 Hz and filtered using a second-order digital Butterworth band-pass filter (passed band 20 to 500 Hz). To assess the level of muscle contraction, the RMS of the EMG signal was calculated in sliding windows of 160 ms with 120-ms overlap. The RMS signals were then normalized using the participant's EMG levels at rest and during an MVC. The resulting NormEMG values served as a feedback signal, visually representing the level of contraction.

To acquire EMG data from TAs, a custom-made multichannel sEMG bracelet was developed (Fig. 7E). This bracelet replaced the commercial table-top amplifier to enable integration with the prosthetic hand in closed-loop experiments. The bracelet featured 10 individual channels, each implementing dry active differential amplification to acquire EMG signals and minimize noise before amplification. Before placing the bracelet, the FCR was palpated, and a single channel was positioned atop it. The overall amplification gain was set to 812 V/V. Signals were filtered using a second-order Sallen Key hardware-based low-pass and high-pass filter with cutoff frequencies of 20 and 500 Hz, respectively. An internal microprocessor within the bracelet converted the analog EMG signals to digital data at a sampling frequency of 1 kHz with 12-bit precision. The processing of digital EMG signals followed a similar methodology to that used for EMG signals recorded with the commercial device in AB participants.

The EMG signals and stimulation control were processed in MATLAB (MathWorks, USA) on a central computer with a custom interface. This interface executed real-time control closed loops and calculated stimulation parameters. It featured a virtual environment displaying a visual representation of a cursor moving along a *y* axis, where the limits corresponded to the NormEMG values ranging from 0 to 100%. This visualization was used to indicate to the participant the level of muscle contraction at any given point in time based on the EMG activity.

Table 1. Clinical data of the recruited amputees in this study.

Participant ID	TA1	TA2	TA3	TA4	TA5	TA6	TA7
Gender	Female	Female	Male	Male	Male	Male	Male
Age	37	35	21	54	33	47	62
Dominant	right	right	right	Ambidextrous	right	right	right
Amputation level	Trans-radial	Trans-radial	Trans-radial	Trans-carpal	Trans-radial	Trans-carpal	Trans-radial
Surgery type	Congenital	Traumatic	Congenital	Traumatic	Traumatic	Traumatic	Traumatic
Time of amputation	Congenital	6 years	Congenital	8 years	9 years	5 years	1987
Years using prosthetic	4 years	4 years	1 year	8 years	8 years	2 years	1989
Forearm diameter (cm)	22	22	19	25	29	24.5	22.5
Amputation length (cm)	10	21	7	23	12	17	16

ERRATUM PUBLISHED 31 JULY 2024; SEE FULL TEXT

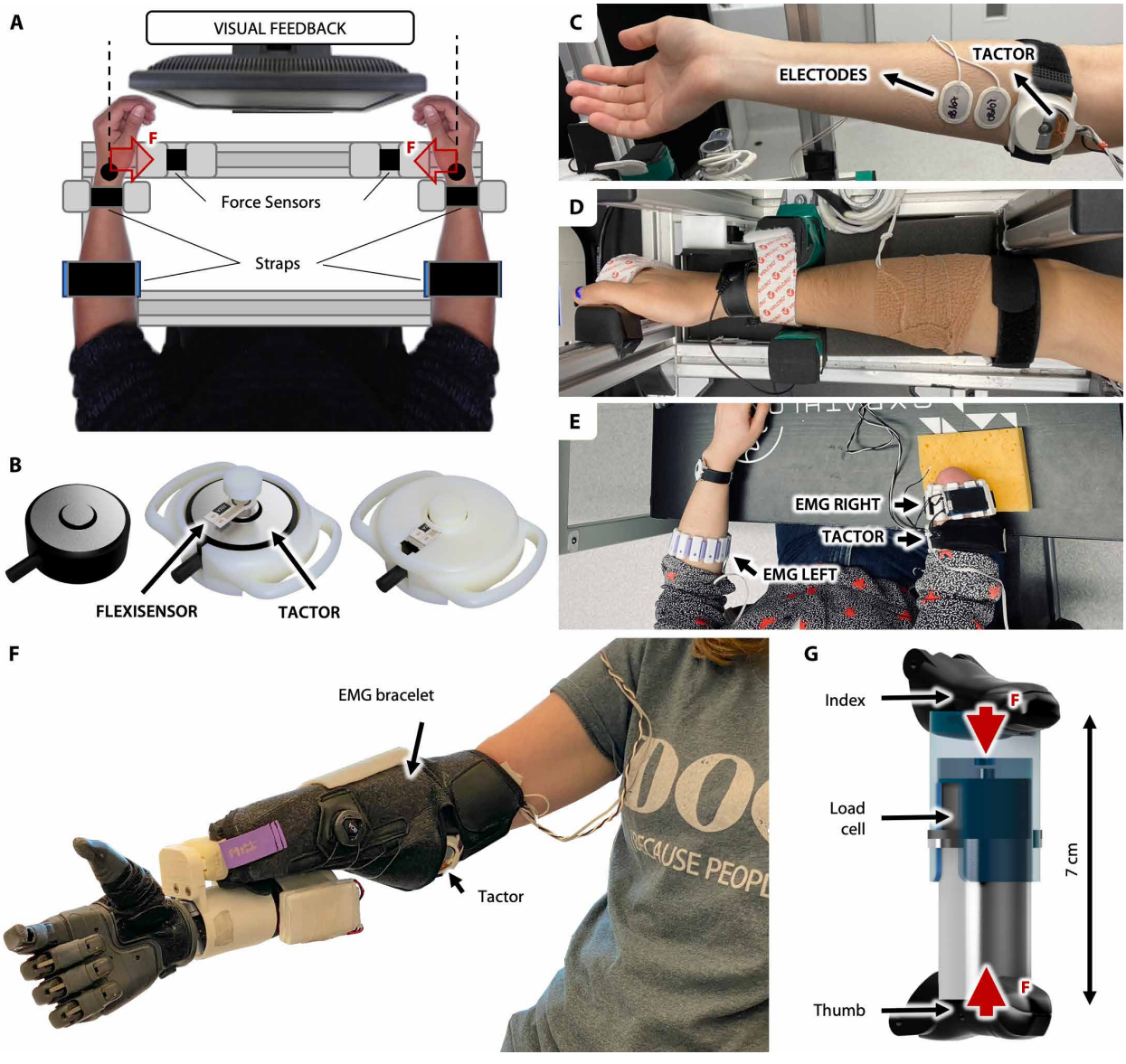

Fig. 7. Experimental setup. (**A**) Force platform setup. Participants sat in front of a computer monitor with their arms strapped in supports to ensure the development of isometric contractions. Participants needed to exert isometric wrist flexion. A force sensor was embedded in the platform hand supports to record the exerted force by the participant. (**B**) Modified stimulator tactor to induce tendon vibration. A force sensor was embedded on the tactor stimulation contact point to measure the perpendicular force to the skin. (**C**) Electrodes and stimulation sites in the experiments with AB participants. (**D**) Forearm arrangement in the force platform to constrain movements and secure isometric wrist flexions. (**E**) Electrodes and stimulation arrangement in the case of TAs. (**F**) Taska prosthesis mounted on the Mitt sleeve by a custom wrist adapter. EMG recording armband and stimulator tactors were in contact with the stump of the participant underneath the sleeve. (**G**) Custom force object for force-tracking tasks. The forces exerted by the hand were concentrated over the load cell shaft located in the center of the cylinder structure.

A commercial hand prosthesis (Taska Prosthetics, New Zealand) was used to implement the reflex-induced feedback. The custom EMG interface and tactor stimulator were embedded on the Mitt sleeve (Koalaa LTD, UK), a soft socket sleeve that fastens with a BOA system (Fig. 7F). A custom adapter was designed to adapt the quick disconnect wrist system of the Taska Hand to the Mitt sleeve. The hand was configured in a pinch grip mode for object interaction, with the pinch aperture controlled by proportionally mapping the EMG output of the target stimulated muscle to the grip range of motion.

For the functional tasks with the prosthesis, a custom force-sensing object was developed (Fig. 7G). It consisted of a sliding cylindrical structure with a central load cell (FC2231-0000-0010-L, TE Connectivity, Switzerland). The upper side of the cylinder was adhered to the load cell, concentrating the exerted forces from the hand onto the shaft. The applied forces were perpendicular to the fingertips, with a maximum operating force of 10 lbs. (4.5 kg). The cylinder had a height of 7 cm to optimize the range of forces that the hand could apply to the object.

Physiological evaluation of the TVR

This evaluation took place during the first day for AB participants. The task involved exerting an isometric wrist flexion at 10% of the NormEMG, a level reported in the literature to facilitate TVR effects (*22*). Initially, participants had 5 s of visual feedback to reach and stabilize the 10% NormEMG target. After this period, the visual feedback was disabled, and participants were instructed to maintain a constant muscle contraction level for 20 s. The tendon stimulation started 5 s after the trial started and lasted for 10 s. The tested stimulus frequencies were 0, 80, 100, 120, and 140 Hz, selected on the basis of previous studies (*47*–*49*, *61*), to determine conditions evoking the largest TVR effects. The stimulation amplitude was set to the maximum of the tactor (1.3 mm). Each frequency was presented randomly in two consecutive blocks of five trials (50 trials in total). For amputee participants, we adjusted the physiological evaluation to accommodate their time constraints. On the basis of results from AB participants, we found that the first block of trials (five per frequency) was sufficient to determine the optimal frequency and reduce experimental time for the amputee. Furthermore, the frequency of 80 Hz was excluded to reduce the experimental process because it had the least effect on all healthy participants.

Intermittent closed-loop tasks

To evaluate the afferent modulation of the motor output, we implemented an intermittent closed loop. For AB participants, this test took place on the second day, whereas for amputees, it was conducted on the same day. During the initial phase, all participants had an initial 5-s period with visual feedback enabled to reach an initial 10% NormEMG target. After this period, the trial commenced.

The intermittent closed loop compared the error between a given EMG target reference and the measured EMG levels. This error served as the feedback signal for the closed loop in an on-off fashion, activating when the measured EMG level was below the target and deactivating when it was above the target. The performance of the closed-loop system was evaluated by the ratio of the RMS values between the current EMG and the target level, providing insight into how effectively the closed loop tracks the reference EMG target.

All AB and amputee participants experienced the intermittent closed loop at two stimulation frequencies: optimal (determined in the previous section) and suboptimal. The suboptimal frequency was set at 40 Hz to include a stimulation condition that should not evoke any TVR effect (*63*, *64*). The suboptimal implementation aimed to confirm that the results obtained with the optimal frequency were attributable to TVR effects on motor output. The performance of the optimal and suboptimal intermittent closed-loop conditions was compared with the pure voluntary performance, where participants followed the target EMG displayed in the visual interface. Each condition (voluntary, optimal closed loop, and suboptimal closed loop) was repeated five times.

Proportional closed-loop evaluation

A proportional closed-loop control condition was implemented to evaluate whether the TVR effects could be integrated with the participants' voluntary control. This closed loop was superimposed on the voluntary drive to create positive feedback and modulate the overall level of muscle activation. The closed loop involved setting the stimulation frequency at the optimal value to evoke the TVR effect while proportionally modulating the stimulation amplitude. This stimulation amplitude was linearly mapped from 0 to 100% on the basis of the range of 0 to 25% NormEMG. This proportional range allowed for increasing stimulation amplitude as the exerted EMG increased, encompassing muscle contraction levels at which the TVR was prominent to drive and excite alpha motor neurons (*64*).

The evaluation tasks included following a ramp target with a slope of 0.75% per second for 20 s, starting at a level of 10% NormEMG. This slope was the average EMG increase gradient among participants during stimulation in pilot experiments. After the slope, there was a 5-s plateau at 25% NormEMG. The impact of the proportional closed loop was assessed by the performance of following the target with and without the closed-loop stimulation. This performance was measured by computing the RMSE between the reference trajectory and the exerted EMG. Each condition was repeated five times.

Functional assessment of afferent closed-loop integration within the prosthesis

A linear regressor was implemented to proportionally control the grip opening and closing of the Taska hand in proportion to the RMS activity of the EMG channel corresponding to the FCR. This processing was performed internally by the EMG bracelet microcontroller. Both the intermittent and proportional closed loops were implemented to operate in real time with the prosthesis.

The targeted box and block test were conducted as part of the proportional closed-loop assessment, following the predefined protocol in (*65*). Participants were required to move nine blocks from one compartment to another separated by a partition (movie S1). Each block had a specific target location and order for transport. A successful transportation was achieved when the block lay flat in the target space. As the prosthesis passed over the partition, the task became more challenging because of the increased difficulty of maintaining a stable grasp while elevating the arm. The overall manual dexterity was evaluated by measuring the time taken to successfully transport all nine blocks from one compartment to the other. The number of block slips during transportation served as an indicator of prosthesis control stability.

Statistical analysis

For the physiological experimentation, a repeated-measures analysis of variance (ANOVA) with Tukey's honest significant difference criterion was used for each participant to compare the ΔEMG elicited by the TVR at the proposed stimulation frequencies. The stimulation frequency that produced the highest ΔEMG was selected as the optimal stimulation frequency. For the intermittent closed-loop experimentation, the success rate was calculated and defined as the RMS of the ratio between the current RMS EMG and RMS target level. A repeated-measures ANOVA was used to compare the success rates between the different closed-loop conditions: voluntary, optimal intermittent, and suboptimal intermittent. In the proportional closed-loop experimentation, the RMSE between the actual EMG level and the target EMG was calculated. A repeated-measures ANOVA was used to compare the success rate when the closed loop was enabled or disabled.

Supplementary Materials

This PDF file includes:
Methods
Figs. S1 to S3

Other Supplementary Material for this manuscript includes the following:
Movies S1 and S2
MDAR Reproducibility Checklist

REFERENCES AND NOTES

1. P. P. Vu, A. K. Vaskov, Z. T. Irwin, P. T. Henning, D. R. Lueders, A. T. Laidlaw, A. J. Davis, C. S. Nu, D. H. Gates, R. B. Gillespie, S. W. P. Kemp, T. A. Kung, C. A. Chestek, P. S. Cederna, A regenerative peripheral nerve interface allows real-time control of an artificial hand in upper limb amputees. *Sci. Transl. Med.* **12**, aay2857 (2020).
2. D. G. K. Madusanka, L. N. S. Wijayasingha, R. A. R. C. Gopura, Y. W. R. Amarasinghe, G. K. I. Mann, A review on hybrid myoelectric control systems for upper limb prosthesis, in *2015 Moratuwa Engineering Research Conference* (IEEE, 2015), pp. 136–141.
3. D. Farina, I. Vujaklija, R. Brånemark, A. M. J. Bull, H. Dietl, B. Graimann, L. J. Hargrove, K.-P. Hoffman, H. Huang, T. Ingvarsson, H. B. Janusson, K. Kristjánsson, T. Kuiken, S. Micera, T. Stieglitz, A. Sturma, D. Tyler, R. F. Weir, O. C. Aszmann, Toward higher-performance bionic limbs for wider clinical use. *Nat. Biomed. Eng.* **7**, 473–485 (2023).
4. S. J. Bensmaia, D. J. Tyler, S. Micera, Restoration of sensory information via bionic hands. *Nat. Biomed. Eng.* **7**, 443–455 (2023).
5. S. Raspopovic, G. Valle, F. M. Petrini, Sensory feedback for limb prostheses in amputees. *Nat. Mater.* **20**, 925–939 (2021).
6. S. S. Hsiao, M. Fettiplace, B. Darbandi, Sensory feedback for upper limb prostheses, in *Enhancing Performance for Action and Perception*, vol. 192 of *Progress in Brain Research*, A. Green, C. E. Chapman, J. F. Kalaska, F. Lepore, Eds. (Elsevier, ed. 1, 2011), pp. 69–81.
7. R. Bekrater-Bodmann, Factors associated with prosthesis embodiment and its importance for prosthetic satisfaction in lower limb amputees. *Front. Neurorobot.* **14**, 604376 (2021).
8. E. Biddiss, T. Chau, Upper-limb Prosthetics. *Am. J. Phys. Med. Rehabil.* **86**, 977–987 (2007).
9. J. W. Sensinger, S. Dosen, A review of sensory feedback in upper-limb prostheses from the perspective of human motor control. *Front. Neurosci.* **14**, 345 (2020).
10. A. M. De Nunzio, S. Dosen, S. Lemling, M. Markovic, M. A. Schweisfurth, N. Ge, B. Graimann, D. Falla, D. Farina, Tactile feedback is an effective instrument for the training of grasping with a prosthesis at low- and medium-force levels. *Exp. Brain Res.* **235**, 2547–2559 (2017).
11. M. Isaković, M. Belić, M. Štrbac, I. Popović, S. Došen, D. Farina, T. Keller, Electrotactile feedback improves performance and facilitates learning in the routine grasping task. *Eur. J. Transl. Myol.* **26**, 197–202 (2016).
12. M. Aboseria, F. Clemente, L. F. Engels, C. Cipriani, Discrete vibro-tactile feedback prevents object slippage in hand prostheses more intuitively than other modalities. *IEEE Trans. Neural Syst. Rehabil. Eng.* **26**, 1577–1584 (2018).
13. G. K. Patel, S. Dosen, C. Castellini, D. Farina, Multichannel electrotactile feedback for simultaneous and proportional myoelectric control. *J. Neural Eng.* **13**, 056015 (2016).
14. M. D. Alonzo, S. Dosen, C. Cipriani, S. Member, HyVE: Hybrid vibro-electrotactile stimulation for sensory feedback and substitution in rehabilitation. *IEEE Trans. Neural Syst. Rehabil. Eng.* **22**, 290–301 (2014).
15. M. A. Schweisfurth, M. Markovic, S. Dosen, F. Teich, B. Graimann, D. Farina, Electrotactile EMG feedback improves the control of prosthesis grasping force. *J. Neural Eng.* **13**, 056010 (2016).
16. M. Štrbac, M. Isaković, M. Belić, I. Popović, I. Simanić, D. Farina, T. Keller, S. Došen, Short- and long-term learning of feedforward control of a myoelectric prosthesis with sensory feedback by amputees. *IEEE Trans. Neural Syst. Rehabil. Eng.* **25**, 2133–2145 (2017).
17. T. Gathmann, S. F. Atashzar, P. G. S. Alva, D. Farina, Wearable dual-frequency vibrotactile system for restoring force and stiffness perception. *IEEE Trans. Haptics* **13**, 191–196 (2020).
18. P. G. Sagastegui Alva, S. Muceli, S. F. Atashzar, L. William, D. Farina, Wearable multichannel haptic device for encoding proprioception in the upper limb. *J. Neural Eng.* **17**, 056035 (2020).
19. F. Clemente, M. D'Alonzo, M. Controzzi, B. B. Edin, C. Cipriani, Non-invasive, temporally discrete feedback of object contact and release improves grasp control of closed-loop myoelectric transradial prostheses. *IEEE Trans. Neural Syst. Rehabil. Eng.* **24**, 1314–1322 (2016).
20. D. M. Page, J. A. George, D. T. Kluger, C. Duncan, S. Wendelken, T. Davis, D. T. Hutchinson, G. A. Clark, Motor control and sensory feedback enhance prosthesis embodiment and reduce phantom pain after long-term hand amputation. *Front. Hum. Neurosci.* **12**, 352 (2018).
21. A. Ninu, S. Dosen, S. Muceli, F. Rattay, H. Dietl, D. Farina, Closed-loop control of grasping with a myoelectric hand prosthesis: Which are the relevant feedback variables for force control? *IEEE Trans. Neural Syst. Rehabil. Eng.* **22**, 1041–1052 (2014).
22. A. W. Shehata, M. Rehani, Z. E. Jassat, J. S. Hebert, Mechanotactile sensory feedback improves embodiment of a prosthetic hand during active use. *Front. Neurosci.* **14**, 513550 (2020).
23. R. M. Mayer, A. Mohammadi, Y. Tan, G. Alici, P. Choong, D. Oetomo, Temporal and spatial characteristics of bone conduction as non-invasive haptic sensory feedback for upper-limb prosthesis. *Front. Neurosci.* **17**, 1113009 (2023).
24. M. Markovic, M. A. Schweisfurth, L. F. Engels, T. Bentz, D. Wüstefeld, D. Farina, S. Dosen, The clinical relevance of advanced artificial feedback in the control of a multi-functional myoelectric prosthesis. *J. Neuroeng. Rehabil.* **15**, 28 (2018).
25. P. Svensson, U. Wijk, A. Björkman, C. Antfolk, A review of invasive and non-invasive sensory feedback in upper limb prostheses. *Expert Rev. Med. Devices* **14**, 439–447 (2017).
26. M. D'Alonzo, S. Dosen, C. Cipriani, D. Farina, HyVE-hybrid vibro-electrotactile stimulation-is an efficient approach to multi-channel sensory feedback. *IEEE Trans. Haptics* **7**, 181–190 (2014).
27. P. D. Marasco, J. S. Hebert, J. W. Sensinger, D. T. Beckler, Z. C. Thumser, A. W. Shehata, H. E. Williams, K. R. Wilson, Neurorobotic fusion of prosthetic touch, kinesthesia, and movement in bionic upper limbs promotes intrinsic brain behaviors. *Sci. Robot.* **6**, eabf3368 (2021).
28. S. Raspopovic, M. Capogrosso, F. M. Petrini, M. Bonizzato, J. Rigosa, G. D. Pino, J. Carpaneto, M. Controzzi, T. Boretius, E. Fernandez, G. Granata, C. M. Oddo, L. Citi, A. L. Ciancio, C. Cipriani, M. C. Carrozza, W. Jensen, E. Guglielmelli, T. Stieglitz, P. M. Rossini, S. Micera, Bioengineering: Restoring natural sensory feedback in real-time bidirectional hand prostheses. *Sci. Transl. Med.* **6**, 222ra19 (2014).
29. P. D. Marasco, K. Kim, J. E. Colgate, M. A. Peshkin, T. A. Kuiken, Robotic touch shifts perception of embodiment to a prosthesis in targeted reinnervation amputees. *Brain* **134**, 747–758 (2011).
30. J. A. George, D. T. Kluger, T. S. Davis, S. M. Wendelken, E. V. Okorokova, Q. He, C. C. Duncan, D. T. Hutchinson, Z. C. Thumser, D. T. Beckler, P. D. Marasco, S. J. Bensmaia, G. A. Clark, Biomimetic sensory feedback through peripheral nerve stimulation improves dexterous use of a bionic hand. *Sci. Robot.* **4**, eaax2352 (2019).
31. E. D'Anna, G. Valle, A. Mazzoni, I. Strauss, F. Iberite, J. Patton, F. M. Petrini, S. Raspopovic, G. Granata, R. Di Iorio, M. Controzzi, C. Cipriani, T. Stieglitz, P. M. Rossini, S. Micera, A closed-loop hand prosthesis with simultaneous intraneural tactile and position feedback. *Sci. Robot.* **4**, eaau8892 (2019).
32. J. S. Schofield, C. E. Shell, D. T. Beckler, Z. C. Thumser, P. D. Marasco, Long-term home-use of sensory-motor-integrated bidirectional bionic prosthetic arms promotes functional, perceptual, and cognitive changes. *Front. Neurosci.* **14**, 120 (2020).
33. R. S. Johansson, G. Westling, Influences of cutaneous sensory input on the motor coordination during precision manipulation, in *Somatosensory Mechanisms*, vol. 12 of *Wenner–Gren Center International Symposium Series*, C. von Euler, O. Franzén, U. Lindblom, D. Ottoson, Eds. (Springer, 1984), pp. 249–260.
34. J. Weiler, P. L. Gribble, J. A. Pruszynski, Spinal stretch reflexes support efficient hand control. *Nat. Neurosci.* **22**, 529–533 (2019).
35. J. P. Roll, J. P. Vedel, Kinaesthetic role of muscle afferents in man, studied by tendon vibration and microneurography. *Exp. Brain Res.* **47**, 177–190 (1982).
36. E. Pierrot-Deseilligny, D. Burke, *The Circuitry of the Human Spinal Cord: Its Role in Motor Control and Movement* (Cambridge Univ. Press, 2009).
37. F. Monjo, J. Shemmell, Probing the neuromodulatory gain control system in sports and exercise sciences. *J. Electromyogr. Kinesiol.* **53**, 102442 (2020).
38. D. Burke, H. H. Schiller, Discharge pattern of single motor units in the tonic vibration reflex of human triceps surae. *J. Neurol. Neurosurg. Psychiatry* **39**, 729–741 (1976).
39. J. L. Taylor, P. G. Martin, Voluntary motor output is altered by spike-timing-dependent changes in the human corticospinal pathway. *J. Neurosci.* **29**, 11708–11716 (2009).
40. E. Todorov, Optimality principles in sensorimotor control. *Nat. Neurosci.* **7**, 907–915 (2004).
41. D. J. Bennett, M. Gorassini, A. Prochazka, Catching a ball: Contributions of intrinsic muscle stiffness, reflexes, and higher order responses. *Can. J. Physiol. Pharmacol.* **72**, 525–534 (1994).
42. R. Lee, W. G. Tatton, Long latency reflexes to imposed displacements of the human Wrist: Dependence on duration of movement. *Exp. Brain Res.* **45**, 480–493 (1982).
43. T. E. Twitchell, The automatic grasping responses of infants. *Neuropsychologia* **3**, 247–259 (1965).
44. C. M. Niu, Q. Luo, C. H. Chou, J. Liu, M. Hao, N. Lan, Neuromorphic model of reflex for realtime human-like compliant control of prosthetic hand. *Ann. Biomed. Eng.* **49**, 673–688 (2021).
45. P. D. Marasco, J. S. Hebert, J. W. Sensinger, C. E. Shell, J. S. Schofield, Z. C. Thumser, R. Nataraj, D. T. Beckler, M. R. Dawson, D. H. Blustein, S. Gill, B. D. Mensh, R. Granja-Vasquez, M. D. Newcomb, J. P. Carey, B. M. Orzell, Illusory movement perception improves motor control for prosthetic hands. *Sci. Transl. Med.* **10**, eaao6990 (2018).
46. G. M. Goodwin, D. I. Mccloskey, P. B. C. Matthews, The contribution of muscle afferents to kinaesthesia shown by vibration induced illusions of movement and by the effects of paralysing joint afferents. *Brain* **95**, 705–748 (1972).

47. G. Eklund, K. E. Hagbarth, Normal variability of tonic vibration reflexes in man. *Exp. Neurol.* **16**, 80–92 (1966).
48. L. G. Bongiovanni, K. E. Hagbarth, Tonic vibration reflexes elicited during fatigue from maximal voluntary contractions in man. *J. Physiol.* **423**, 1–14 (1990).
49. D. Burke, K. E. Hagbarth, L. Löfstedt, B. G. Wallin, The responses of human muscle spindle endings to vibration during isometric contraction. *J. Physiol.* **261**, 695–711 (1976).
50. B. M. C. Brown, I. Engberg, P. B. C. Matthews, The relative sensitivity to vibration of muscle receptors of the cat. *J. Physiol.* **44**, 773–800 (1967).
51. J. B. Fallon, V. G. Macefield, Vibration sensitivity of human muscle spindles and golgi tendon organs. *Muscle Nerve* **36**, 21–29 (2007).
52. F. Lacquaniti, Transient reversal of the stretch reflex in human arm muscles. *J. Neurophysiol.* **66**, 939–954 (1991).
53. C. Shi, D. Yang, J. Zhao, H. Liu, Computer vision-based grasp pattern recognition with application to myoelectric control of dexterous hand prosthesis. *IEEE Trans. Neural Syst. Rehabil. Eng.* **28**, 2090–2099 (2020).
54. M. Markovic, S. Dosen, D. Popovic, B. Graimann, D. Farina, Sensor fusion and computer vision for context-aware control of a multi degree-of-freedom prosthesis. *J. Neural Eng.* **12**, 066022 (2015).
55. M. Tawfik, I. A. Baqer, A. Abdulsahib, Grasping force controlling by slip detection for specific artificial hand (Ottobock 8E37). *Eng. Technol. J.* **36**, 979–984 (2018).
56. P. Kyberd, Slip detection strategies for automatic grasping in prosthetic hands. *Sensors* **23**, 4433 (2023).
57. N. Thomas, F. Fazlollahi, J. D. Brown, K. J. Kuchenbecker, Sensorimotor-inspired tactile feedback and control improve consistency of prosthesis manipulation in the absence of direct vision, in *IEEE/RSJ International Conference on Intelligent Robots and Systems (IROS)* (IEEE, 2021), pp. 6174–6181.
58. M. N. Castro, S. Dosen, Continuous Semi-autonomous prosthesis control using a depth sensor on the hand. *Front. Neurorobot.* **16**, 814973 (2022).
59. D. Burke, K. E. Hagbarth, L. Löfstedt, B. G. Wallin, The responses of human muscle spindle endings to vibration of non-contracting muscles. *J. Physiol.* **261**, 673–693 (1976).
60. J. P. Roll, J. P. Vedel, E. Ribot, Alteration of proprioceptive messages induced by tendon vibration in man: A microneurographic study. *Exp. Brain Res.* **76**, 213–222 (1989).
61. P. Romaiguère, J. P. Vedel, S. Pagni, Effects of tonic vibration reflex on motor unit recruitment in human wrist extensor muscles. *Brain Res.* **602**, 32–40 (1993).
62. J. Luo, B. P. McNamara, K. Moran, A portable vibrator for muscle performance enhancement by means of direct muscle tendon stimulation. *Med. Eng. Phys.* **27**, 513–522 (2005).
63. H. S. Park, B. J. Martin, Contribution of the tonic vibration reflex to muscle stress and muscle fatigue. *Scand. J. Work. Environ. Heal.* **19**, 35–42 (1993).
64. B. J. Martin, H. S. Park, Analysis of the tonic vibration reflex: Influence of vibration variables on motor unit synchronization and fatigue. *Eur. J. Appl. Physiol. Occup. Physiol.* **75**, 504–511 (1997).
65. K. Kontson, I. Marcus, B. Myklebust, E. Civillico, Targeted box and blocks test: Normative data and comparison to standard tests. *PLOS ONE* **12**, e0177965 (2017).
66. Taska Prosthetics (2023); www.taskaprosthetics.com.

Acknowledgments

Funding: This study was funded by the European Research Council (Synergy Grant 20 Natural BionicS, contract no. 810346). J.P. was supported by a Ramón y Cajal grant (RYC2021-031905-I) and a Consolidación Investigadora grant (CNS2022-135366) funded by MCIN/AEI/10.13039/501100011033 and UE's NextGenerationEU/PRTR funds. **Author contributions:** Conceptualization: P.G.S.A., J.I., D.F., and O.C.A. Methodology: P.G.S.A., J.I., and D.F. Investigation: P.G.S.A., J.I., D.F., and A.B. Visualization: P.G.S.A. Funding acquisition: D.F. and O.C.A. Supervision: J.I., D.F., and O.C.A. Writing—original draft: P.G.S.A. Writing—review and editing: J.I., D.F., O.C.A., and A.B. **Competing interests:** The authors declare that they have no competing interests. **Data and materials availability:** All data needed to evaluate the conclusions in this paper are present in the paper or the Supplementary Materials.

Submitted 23 September 2023
Accepted 30 April 2024
Published 29 May 2024
10.1126/scirobotics.adl0085

Science Robotics

Excitation of natural spinal reflex loops in the sensory-motor control of hand prostheses

Patrick G. Sagastegui Alva, Anna Boesendorfer, Oskar C. Aszmann, Jaime Ibáñez, and Dario Farina

Sci. Robot. **9** (90), eadl0085. DOI: 10.1126/scirobotics.adl0085

Editor's summary
Restoring sensory feedback in amputees is necessary to improve prosthesis control, but several noninvasive techniques to achieve this are cognitively demanding. Sagastegui Alva *et al*. developed a closed-loop feedback approach to aid prosthesis control by stimulating spinal motor neurons through mechanical vibration of tendons. The system was tested with trans-radial amputees and showed the ability to improve functional motor skills, including grasping dexterity, with a prosthesis device. The study demonstrates the potential of using both voluntary and involuntary action with natural feedback loops to control prostheses. —Amos Matsiko

Science Robotics (ISSN 2470-9476) is published by the American Association for the Advancement of Science. 1200 New York Avenue NW, Washington, DC 20005. The title *Science Robotics* is a registered trademark of AAAS.